COO/2617-76/1/1
Distribution Category UC-60

FEASIBILITY INVESTIGATION OF THE GIROMILL FOR GENERATION OF ELECTRICAL POWER

VOLUME I - EXECUTIVE SUMMARY

Final Report for the
Period April 1975 - April 1976

R.V. Brulle

MCDONNELL AIRCRAFT COMPANY
Box 516
St. Louis, Missouri 63166

Date Published - January 1977

PREPARED FOR THE UNITED STATES
ENERGY RESEARCH AND DEVELOPMENT ADMINISTRATION
DIVISION OF SOLAR ENERGY

Under Contract No. EY-76C-02-2617.A001

Available from the National Technical Information Service, U. S. Department of Commerce, Springfield, Virginia 22161.

Price: Paper Copy \$4.50
Microfiche \$3.00

FOREWORD

This report was prepared for the United States Energy Research and Development Administration (ERDA) by the McDonnell Aircraft Company (MCAIR), a division of the McDonnell Douglas Corporation, P.O. Box 516, St. Louis, Missouri 63166. This study was performed under ERDA contract E(11-1)-2617.

This final report covers the results obtained over the entire contract period from 1 April 1975 to 30 April 1976. However, emphasis is given to the period subsequent to the publication of our mid-term report on 1 November 1975. The pertinent results from the mid-term are summarized so that this final report is complete and can stand alone. In addition, the contents of this report are arranged in the same order as our mid-term to make cross checking and referencing between them convenient. The report is in two volumes. Volume I is an Executive Summary and Volume II the Technical Discussion.

The study was under the direction of Robert V. Brulle. Contributing personnel were: William E. Simon and R. D. Turner, aerodynamics and performance; Thomas V. Hinkle and Anthony R. Dill, structural strength analysis; Rudy N. Yurkovich, structural dynamics; Bruno Fajfar, control system; Fred R. Cole and John J. Blommer, design; Robert A. Juergens, electronics; and James H. Carlson, costs.

ABSTRACT

The Giromill (from cyclogiro windmill) consists of a number of vertical blades rotating around a central tower. The blades angle of attack are individually modulated to achieve high wind energy conversion efficiency. This one year study concentrated on determining the feasibility of the Giromill for the cost effective production of electrical energy.

Twenty-one different Giromill configurations covering three sizes of Giromill systems (120, 500 and 1500 kW) were analyzed, varying such parameters as rotor solidity, rotor aspect ratio, rated wind velocity, and number of rotor blades. The Giromill system analysis employed the same ground rules being used for conventional windmill analyses to facilitate comparisons between these systems.

The results indicate that a Giromill is a very efficient device, and coupled with its relatively simple construction appears quite cost effective when compared to conventional windmills. A 500 kW Giromill system, placed in a 5.4 mps mean wind site, can generate electrical power for 4.05¢ per kW hr. which is 18 to 39% less than that of conventional windmills. Further effort to verify the analytical performance with a wind tunnel test is recommended.

TABLE OF CONTENTS

LIST OF ILLUSTRATIONS

1. OVERVIEW

The Giromill (from cyclogiro windmill) consists of a number of vertical blades rotating around a central tower. The blades rock angles are individually modulated to achieve high wind energy conversion efficiency. This one year ERDA sponsored study concentrated on determining the feasibility of the Giromill for cost effective production of electrical energy.

Figure 1 shows a typical 500 kW Giromill configuration. It has 3 symmetrical constant chord blades, each having a chord (c) of 1.65 meters and a full span (b) of 29.7 meters. The blade modulation actuator is placed at mid span. The blades are attached to the central tower with 3 blade support arms providing a 62.3 meter rotor diameter (D). This results in a rotor aspect ratio (AR_R = b/D) of 0.476, and a rotor solidity (σ = no. of blades x c/D) of 0.079. The blade speed ratio (λ = blade rotational speed/wind speed) is 3.85 when the power coefficient (C_P) is a maximum. This Giromill is sized for placement in a 5.4 mps mean wind ($\overline{V}$) site, and has a rated wind speed (V_R) of 8.1 mps.

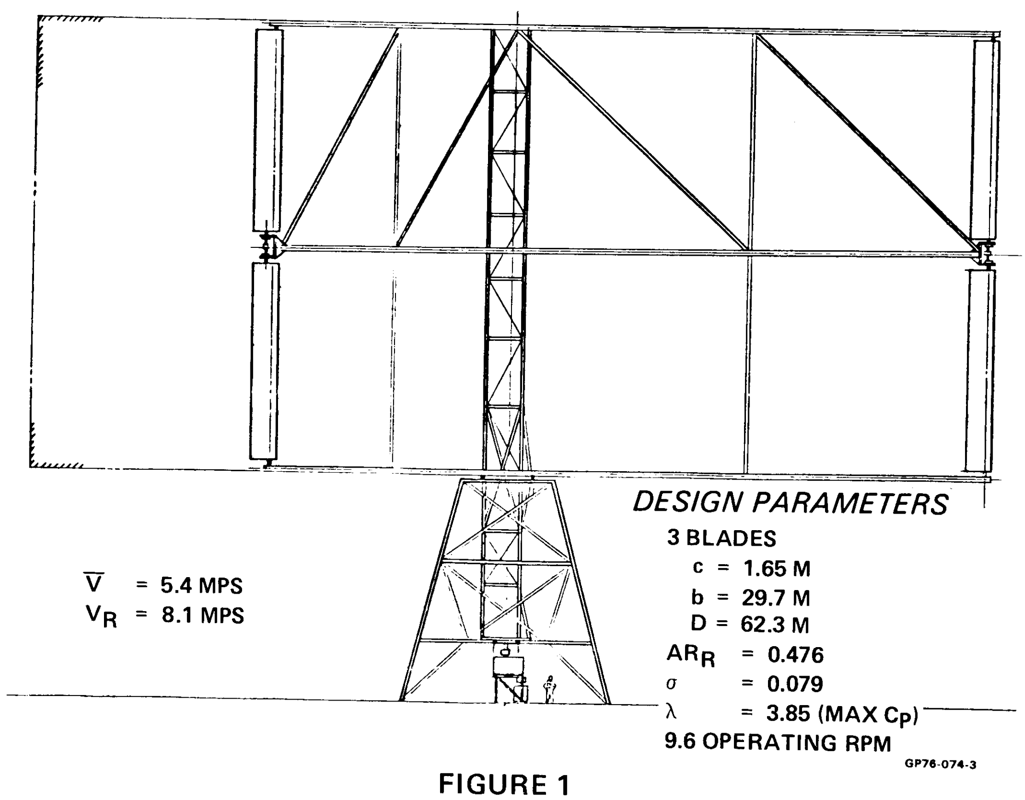

FIGURE 1
GIROMILL CONFIGURATION
500 kW

The study plan followed is shown in Figure 2. Twenty one different Giromill configurations covering three sizes of Giromill systems were analyzed, varying such parameters as rotor solidity, rotor aspect ratio, rated wind velocity, and number of rotor blades. The performance, design, and cost effectiveness of these 21 configurations were determined. The results of this analysis formed the base for selecting a configuration that was optimized for the least cost of energy. The Giromill configuration depicted in Figure 1 is this optimized system.

- AERODYNAMIC PERFORMANCE ANALYSIS USING LARSEN CYCLOGIRO VORTEX THEORY COMPUTER PROGRAM
- PRELIMINARY DESIGN OF 21 DIFFERENT GIROMILL CONFIGURATIONS - 120, 500 AND 1500 kW
- COST EFFECTIVE ANALYSIS
- OPTIMIZATION OF MOST COST EFFECTIVE CONFIGURATION
- PREPARATION OF NEXT PHASE WIND TUNNEL TEST PLAN

GP76-374-2

FIGURE 2
STUDY PLAN FOLLOWED

2. GIROMILL CONFIGURATIONS SELECTED

The pertinent design ground rules employed are shown in Figure 3. To facilitate comparison these ground rules are similar to those used for conventional windmill studies. For expediency of this feasibility study, the generator and RPM speed increaser efficiency was held constant.

Figure 4 summarizes the physical characteristics of the 21 Giromill configurations studied. Note that all 120 and 500 kW configurations studied had 3 blades. Only the 1500 kW system considered the effect of more blades. A Giromill configuration having two blades was initially investigated but was discarded in favor of a 3 bladed configuration. Three blades produces a positive torque at all points on the rotor orbit, assures starting with the wind from any direction, and has better structural dynamic properties.

- CONSTANT ROTOR RPM WITH SYNCHRONOUS GENERATOR
- MEAN WIND $\overline{V}$ = 5.4 MPS FOR 120 AND 500 kW SYSTEMS AND 8.1 MPS FOR 1500 kW SYSTEM
- STATIC COMPONENTS DESIGN LIFE OF 50 YEARS
- DYNAMIC COMPONENTS DESIGN LIFE OF 30 YEARS
- WITHSTAND WIND GUSTS TO 27 MPS OPERATING
- WITHSTAND WINDS TO 54 MPS WITH BLADES FREE
- GENERATOR EFFICIENCY 95%
- RPM SPEED INCREASER EFFICIENCY 96%

GP76-0374-4

FIGURE 3
DESIGN GROUND RULES

Configuration		Rated Velocity mps	Number of Blades	RPM	Rotor Solidity	Rotor Aspect Ratio	Rotor Diameter Meters	Rotor Span Meters	Rotor Blade Chord Meters
120 kW	1	8.05	3	27.0	0.159	1.073	20.4	21.9	1.08
	2	8.05	3	24.0	0.198	1.073	20.4	21.9	1.35
	3	8.05	3	21.3	0.238	1.073	20.4	21.9	1.62
	4	8.05	3	20.0	0.198	0.746	24.5	18.3	1.62
	5	8.05	3	26.0	0.198	0.477	30.6	14.6	2.02
	6	7.15	3	18.0	0.198	1.073	24.3	26.1	1.61
	7	8.94	3	31.5	0.198	1.073	17.4	18.7	1.15
500 kW	8	8.05	3	17.7	0.079	1.073	43.0	46.2	1.14
	9	8.05	3	15.1	0.119	1.073	43.0	46.2	1.71
	10	8.05	3	12.8	0.159	1.073	43.0	46.2	2.26
	11	8.05	3	11.8	0.079	0.477	64.6	30.8	1.71
	12	8.05	3	11.5	0.119	0.614	56.9	34.9	2.26
	13	7.15	3	11.3	0.119	1.073	51.3	56	2.04
	14	8.94	3	19.7	0.119	1.073	36.7	39.4	1.46
	15	8.05	3	10.1	0.238	1.073	43.0	46.2	3.41
	16	8.05	3	13.5	0.119	0.85	48.3	40.8	1.92
1500 kW	17	11.6	3	18.5	0.159	1.073	43	46.2	2.26
	18	11.6	3	14.6	0.238	1.073	43	46.2	3.41
	19	11.6	3	12.7	0.317	1.073	43	46.2	4.54
	20	11.6	4	14.2	0.238	1.073	43	46.2	2.56
	21	11.6	5	14.6	0.238	1.073	43	46.2	2.04

GP77-0007-56

FIGURE 4
GIROMILL STUDY CONFIGURATIONS

3. PERFORMANCE

The performance characteristics of the Figure 1 Giromill configuration are shown in Figure 5. The effective angle of attack (α_e) referred to in the figure is the nominal commanded value, either positive or negative, around the blade orbit. The actual value varies due to rotor vortex effects and the smoothing of the blade modulation rock angle by the control system. Figure 6 presents the performance results, determined utilizing the Larsen cyclogiro vortex theory.

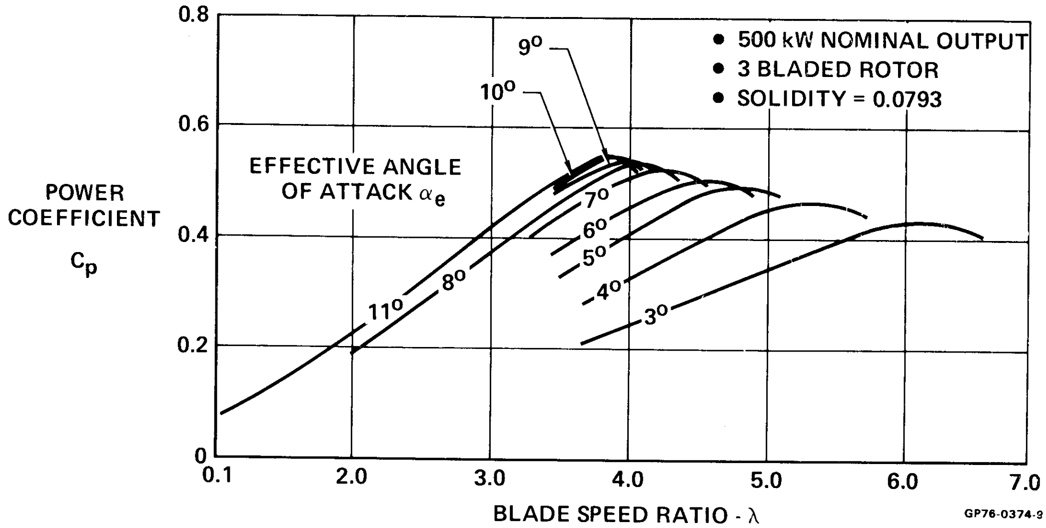

FIGURE 5
GIROMILL PERFORMANCE CHARACTERISTICS

- POWER OUTPUT INDEPENDENT OF ROTOR ASPECT RATIO (AR_R)
- ROTOR POWER IS PROPORTIONAL TO CAPTURE AREA
- RPM VARIES INVERSELY WITH ROTOR DIAMETER FOR GIVEN POWER
- OPTIMUM RPM VARIES INVERSELY WITH SOLIDITY
- MAXIMUM ROTOR EFFICIENCY IS INDEPENDENT OF NUMBER OF BLADES AND SOLIDITY
- LOW SOLIDITY FLATTENS THE POWER CURVE AT HIGH BLADE SPEED RATIOS
- FOR GIVEN POWER AND SOLIDITY, RPM VARIES DIRECTLY WITH RATED WIND SPEED

GP76-0374-8

FIGURE 6
PERFORMANCE RESULTS

4. DESIGN ANALYSIS

Various Giromill conceptual designs were investigated as shown in Figure 7. Concept (A) was the original design shown in the June 1975 Wind Energy Workshop Proceedings. The Giromill structural dynamics due to the cable sag and sway, the increased load in the lower bearing due to cable tension, the requirement for the large stiff cable support arms, and the large area of real estate required for the cable tie down were the negative aspects of this type of design. The fixed tower design shown in (B) appeared attractive except for providing a power drive to the generator. There appeared to be no cost effective method of transmitting the rotor torque to a generator drive shaft. Using a single ring and pinion gear at the bottom or middle blade support requires that the entire rotor torque be directed through that gear. This requires a heavy blade support structure. Three ring gears (one at each blade support) could be used, however, the mechanical complexity and the long drive shaft are the negative aspects. Concept (C) was the design selected for this feasibility study, and consists of a simple structural built-up rotating upper tower cantilevered from the lower stationary tower. Two main rotor bearings react the tipping moment. The lower bearing also reacts the rotor weight. A descriptive sketch of this concept is shown in Figure 8.

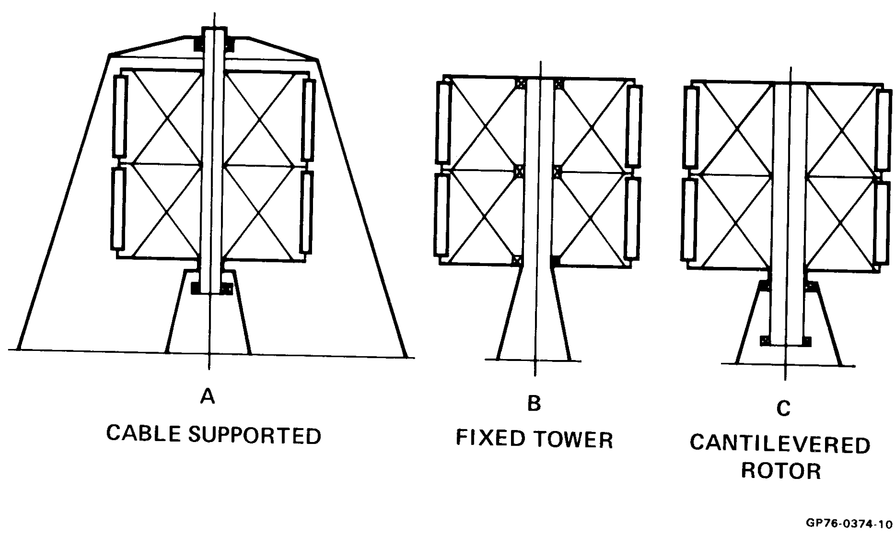

FIGURE 7
CONCEPTUAL DESIGNS INVESTIGATED

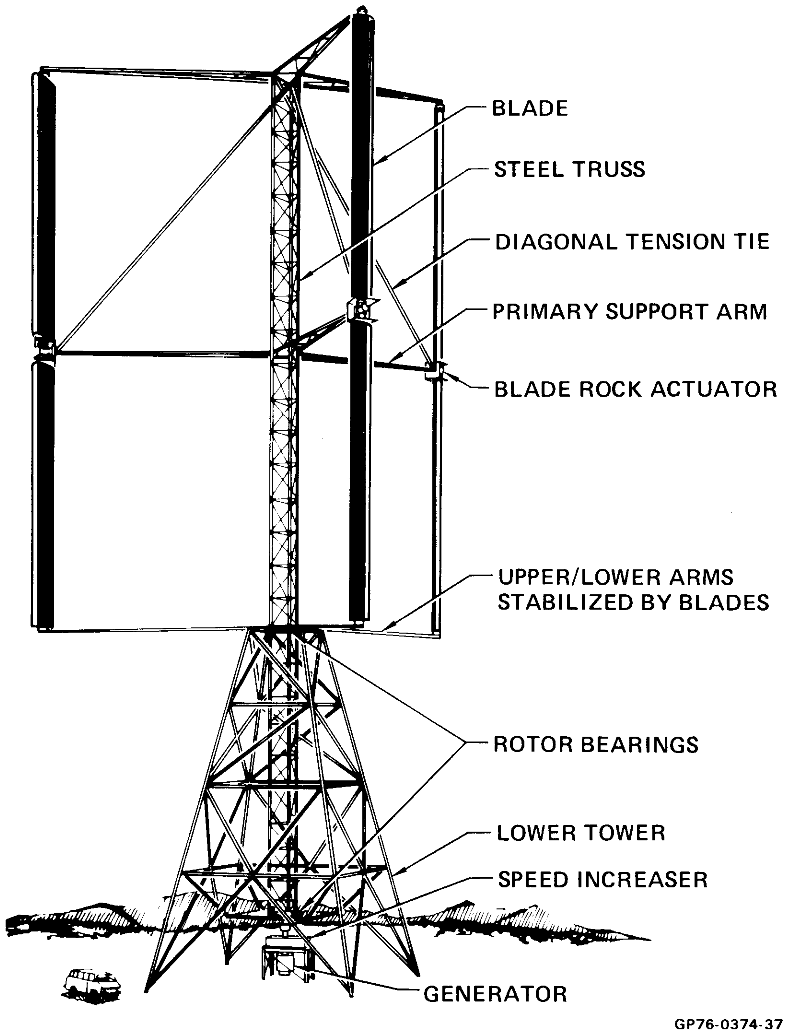

FIGURE 8
FINAL CONFIGURATION

Blade concepts investigated are shown in Figure 9. Concept (A) had initially shown promise because of its ease of manufacture since it had no ribs. It had, however, a relatively high polar moment of inertia and required considerable ballast to locate the CG at the pivot point (25% chord). Concept (B) had an extruded leading edge torque box with a sheet trailing edge stabilized by sheet metal ribs fastened to the leading edge extrusion. It was found that a closed "D" type extrusion as shown was expensive and not very practical. Two extrusions, a leading edge and a spar in place of the "D" extrusion was also evaluated, but was still not as attractive as concept (C). Because the blades are symmetrical and have a constant chord they lend themselves to the rolling and brake forming of the leading edge and spar, and constructing as shown in (C). This blade concept was used for the Giromill design analysis.

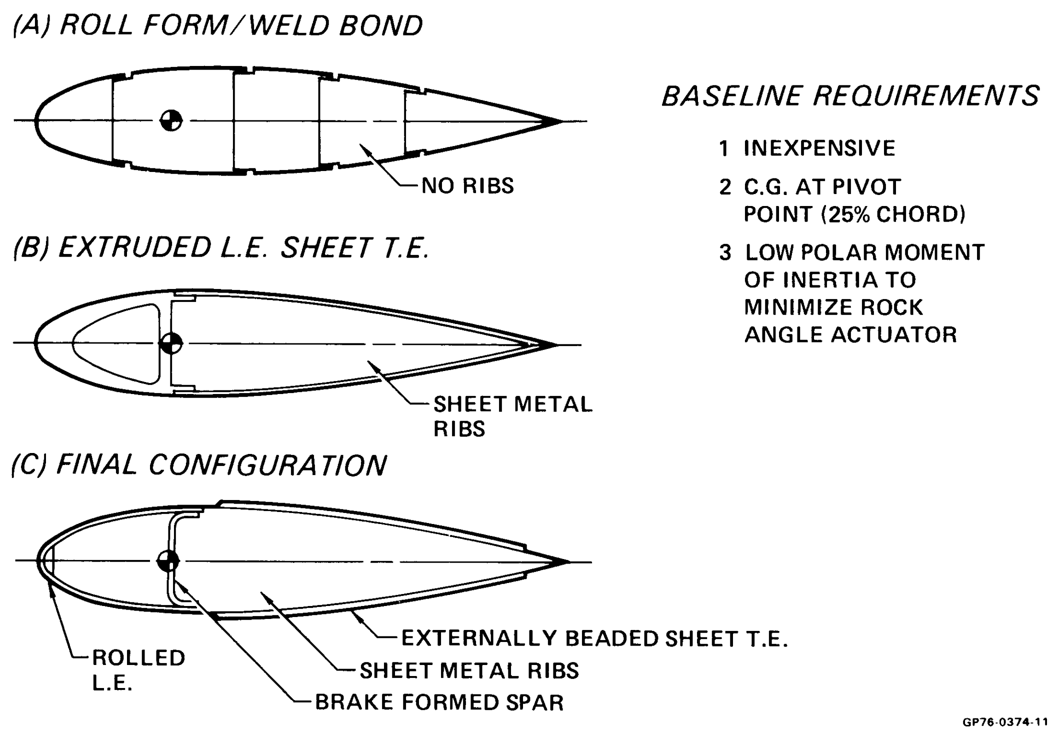

FIGURE 9
BLADE CONCEPTS INVESTIGATED

The generator drive systems looked at are summarized in Figure 10. A ring and pinion gear around the upper tower by the lower main bearing was found to provide an insufficient RPM increase to drive the generator directly and a low ratio speed increaser was still required. The cost for the large ring gear and low ratio speed increaser was greater than for a high ratio speed increaser by itself, hence this concept was discarded. The large diameter of a Giromill's rotor structure could be used to provide a peripheral track for a friction drive wheel attached directly to the generator. Friction drives have been used with obvious success in automobiles and railroad systems, but have not proven suitable in many industrial applications. A friction drive, although attractive for larger high power type Giromills, would require testing and verification before use. For this feasibility analysis this concept was not considered further, and a conventional commercially available RPM speed increaser was used.

Figure 11 shows a sketch of the blade rock angle actuator concept. The rotary actuator is a brushless DC motor driving through an electrical clutch to a speed reducer to the blade. The critical life cycle component was determined to be the bearings. The 120 kW systems required an actuator having a maximum power output of 0.6 HP; the 500 kW required 5 HP, and the 1500 kW 15 HP.

- RING/PINION GEAR AROUND MAIN BEARING
  - RPM INCREASE INSUFFICIENT
  - STILL REQUIRED A RPM SPEED INCREASER
- FRICTION DRIVE AROUND A ROTOR-MOUNTED PERIPHERAL TRACK
  - FEASIBLE BUT NEEDS VERIFICATION
  - ESPECIALLY ATTRACTIVE FOR LARGE HIGH POWER GIROMILLS
- CONVENTIONAL RPM SPEED INCREASER

GP76-0374-12

FIGURE 10
GENERATOR DRIVE SYSTEMS INVESTIGATED

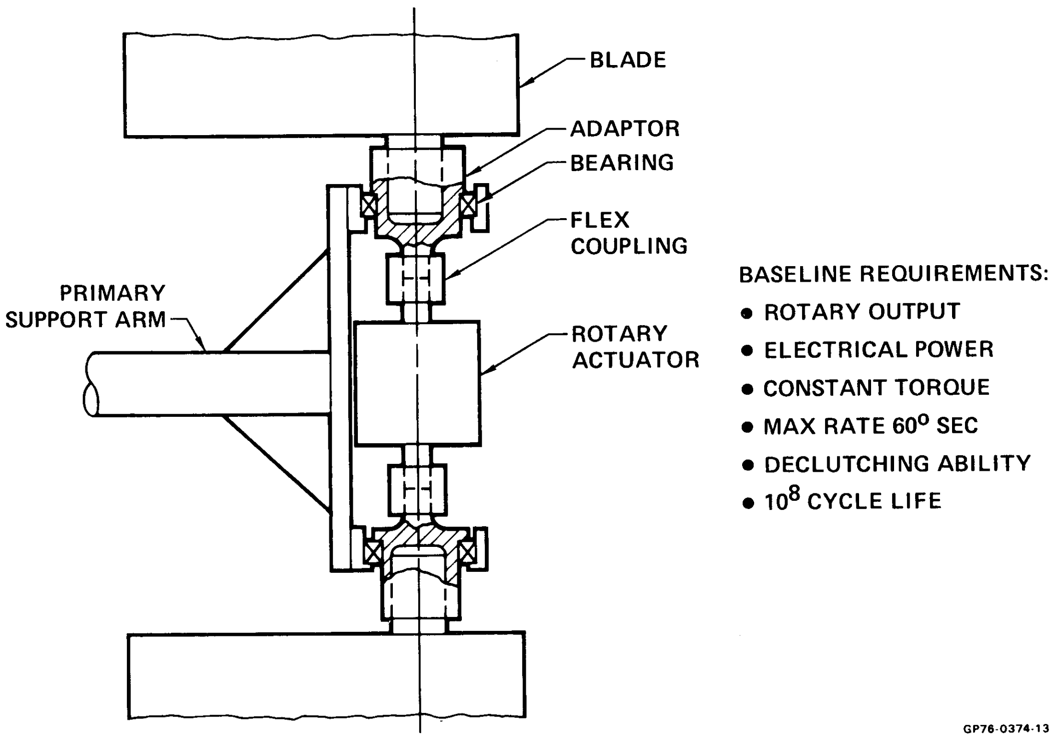

FIGURE 11
BLADE ROCK ANGLE ACTUATOR

5. STRUCTURAL ANALYSIS

The structural arrangement of the Giromill was studied as three sub-structures: (1) blades, (2) blade supports, and (3) tower (both upper and lower). Each of these sub-structures were sized using the structural design criteria shown in Figure 12. The loading conditions used in the sizing were: (1) normal operation under rated conditions, (2) operating under wind gust conditions, and (3) non operating (blades declutched) in high winds.

- NO STRUCTURAL FAILURE UNDER DESIGN ULTIMATE LOADS
- SERVICE LIFE OF DYNAMIC COMPONENTS 30 YEARS, 10^8 CYCLES OF DESIGN LIMIT LOADS
- DESIGN LIMIT LOADS = MAXIMUM EXPECTED LOADS
- ULTIMATE LOADS = FS x LIMIT LOADS
  - BLADES FS = 2.0
  - BLADE SUPPORTS AND TOWER FS = 3.0

GP76-0374-14

FIGURE 12
STRUCTURAL DESIGN CRITERIA

A typical blade limit load cycle used for the blade design is presented in Figure 13. The design of the blades was found to be dictated by the service life requirements. As such, the peak loads associated with normal operation under rated conditions becomes the design loads since the gust wind condition occurs too infrequently to cause fatigue failure. The inertial or centrifugal load component loads the blade sufficiently to prevent a blade load reversal.

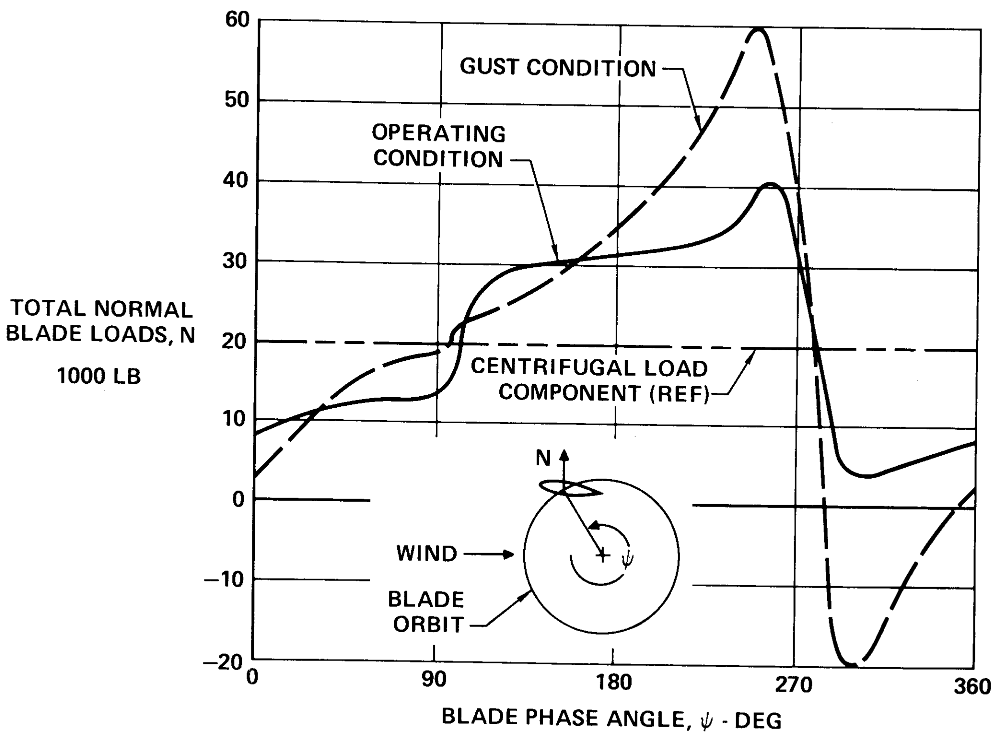

GP76-0374-15

FIGURE 13
BLADE LIMIT LOADS

An aluminum alloy was selected for the blade material. In addition to the high structural efficiency of aluminum relative to other common materials such as steel, aluminum is easily formed, naturally resistant to galvanic corrosion and the selected alloy, 2024-T6 exhibits good resistance to stress corrosion. The endurance limit of this aluminum, for an assumed stress ratio of zero, and a stress concentration factor of 2.81 which represents a mechanical fastener construction, is 14000 PSI. These blade design characteristics are shown in Figure 14.

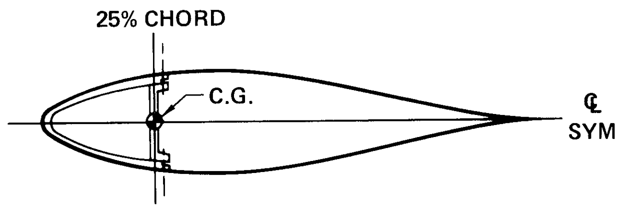

- MATERIAL: ALUMINUM, 2024-T6
- BLADE DESIGN: 30-YEAR SERVICE LIFE
  - LOADS - NORMAL OPERATING CONDITION
  - ALLOWABLE STRESS -

    STRESS RATIO 0
    STRESS CONCENTRATION 2.81 } (14 KSI)
    ENDURANCE LIMIT

GP76-0374-16

FIGURE 14
BLADE DESIGN CHARACTERISTICS

The blade supports and upper and lower tower are dictated by both the service life and ultimate load criteria. Commercial steels were selected for these substructures. These substructures are basically compression structures sized to ultimate loads from the storm wind condition; however, members designed to these loads, in general, exhibit limit (expected) operating stresses which exceed fatigue allowables at the member splices. These joints were beefed-up to reduce the operating stresses to an acceptable level. The allowable fatigue of mechanically fastened carbon steel joints is based on 10^9 load cycles and a stress ratio conservatively assumed to be -1.0.

The Giromill system total weight for the 120 and 500 kW systems is shown as a function of rotor aspect ratio in Figure 15. These typical data indicate that low rotor aspect ratio systems have a lower total weight and, more important, that the 500 kW system produces more power per unit weight in the same wind environment (for a weight increase of 223% the power is increased 317%). The structural weight analysis results are tabulated in Figure 16. Note the inclusion of configuration 11-1 which was optimized for lower energy cost.

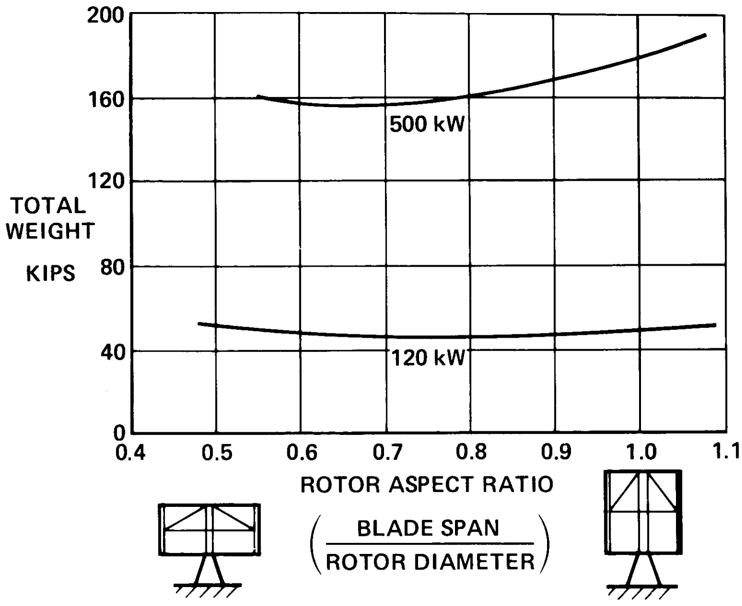

FIGURE 15
LARGER GIROMILLS PRODUCE MORE
POWER PER UNIT WEIGHT

CONFIGURATION		BLADE WEIGHTS (LB)	BLADE SUPPORT WEIGHTS (LB)	UPPER TOWER WEIGHT (LB)	LOWER TOWER WEIGHT (LB)	TOTAL SYSTEM WEIGHT (LB)
120 kW	1	5,430	8,220	19,280	18,050	50,980
	2	4,230	8,330	19,280	18,050	49,480
	3	4,750	8,390	19,280	18,050	50,470
	4	3,950	12,430	14,220	16,800	47,400
	5	3,950	21,050	10,830	16,450	52,280
	6	5,830	13,190	29,300	21,050	69,370
	7	3,200	5,500	13,390	15,950	38,040
500 kW	8	13,960	38,780	90,790	36,700	180,230
	9	16,960	37,060	98,000	36,800	188,820
	10	14,800	36,970	98,000	36,800	186,570
	11	7,350	79,100	43,180	26,750	156,380
	11-1 (OPTIMIZED)	14,500	57,100	31,200	28,800	131,600
	12	10,930	60,760	54,350	29,200	155,240
	13	19,330	58,750	154,480	46,200	278,760
	14	15,730	24,060	65,540	30,400	135,630
	15	21,280	45,260	117,370	37,950	221,860
	16	NOT COMPLETED				
1500 kW	17	15,460	46,210	91,700	36,990	190,360
	18	24,300	60,350	99,380	37,210	221,240
	19	32,330	65,600	100,280	37,490	235,700
	20	23,830	78,400	101,260	37,780	241,270
	21	28,190	95,930	100,500	37,540	262,160

GP76-0374-38

FIGURE 16
GIROMILL WEIGHTS

6. STRUCTURAL DYNAMICS

The purpose of the structural dynamics investigation was to determine frequencies and associated mode shapes of the Giromill vibrations, determine those that are critical, and then identify the problems associated with tuning the critical vibrations to alleviate their criticality.

Figure 17 presents a typical result of a Giromill system structural dynamics analysis. Of all modes identified only the upper tower torsion and bending appeared critical. The blade torsion frequency was not computed since the blade actuator stiffness was not defined. A cursory look using an expected range of blade actuator stiffness values indicated the blade torsion would be satisfactory.

MODE	NATURAL FREQUENCY (Hz)
UPPER TOWER TORSION	0.22
UPPER TOWER BENDING	0.34
BLADE TORSION	TORSIONAL SUPPORT UNDEFINED
SUPPORT ARM TANGENTIAL BENDING (IN PHASE, LAG-LEAD ARM BENDING)	1.88
BLADE FLAP BENDING	3.93
SUPPORT ARM VERTICAL BENDING (OUT OF PHASE)	5.12
SUPPORT ARM TANGENTIAL BENDING (OUT OF PHASE)	3.39
SUPPORT ARM TANGENTIAL BENDING (IN PHASE, BLADE MODE)	4.23
SUPPORT ARM VERTICAL BENDING (IN PHASE)	2.96

GP76-0374-18

FIGURE 17
STRUCTURAL DYNAMICS FREQUENCIES
500 kW Configuration 11-1

Figure 18 presents a Campbell diagram showing the tower bending and torsion modes, and how they react with the various excitation frequencies. The points of strong forced vibrations are indicated by the circled symbols. The operating rotational speed does not pass through any of the force vibration points, but is close to several. Note also that starting and stopping the Giromill will require passing through several others. The structural ramifications of these resonant frequencies was not considered in this feasibility analysis. The structural dynamics criteria stipulated was that the natural frequencies and forcing excitations be reasonably separated and that no aeroelastic instabilities exist.

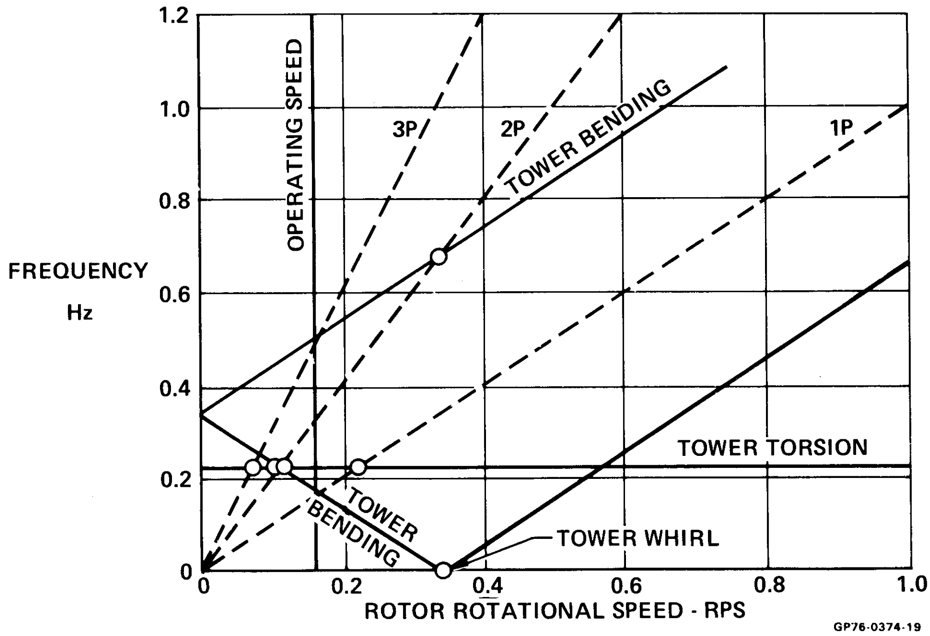

FIGURE 18
TOWER DYNAMICS
500 kW Configuration 11-1

The tower can be tuned to provide acceptable dynamic response characteristics. The corner members of the tower primarily affect the tower bending frequency and the cross members the torsion frequency. Tower diameter also strongly influences the dynamics. The interplay of these three parameters indicated a large range of tower dynamics could be achieved without significantly affecting the tower weight.

7. CONTROL SYSTEM

The main functional requirement of the control system is to enable the Giromill to generate the maximum rated power output without exceeding the structural and electrical load limitations. The control system performs this function by controlling the blade rock angles so that the desired Giromill power output is maintained in the presence of wind variations. Other control system functions provide for the startup and power interrupt or shutdown situations as they occur to insure that safe operating conditions are met.

An electronic control system was selected for this feasibility study since it appeared easier to implement at this time than a mechanical system. Figure 19 presents a simplified control system functional diagram. The sensor signals include such parameters as: the wind velocity and direction, rotor RPM, blade phase angle, vibration level, and electrical power conditions. On the basis of the values of these parameters the control system provides the logic to completely control the Giromill. The blade angle computations block in Figure 19 provides the command (Θ_{R_C}) to the blade rock angle actuators. The actuators respond and provide a rock angle (Θ_R) to the blades. The aerodynamic forces on the blades cause the rotor to turn, generating a power output.

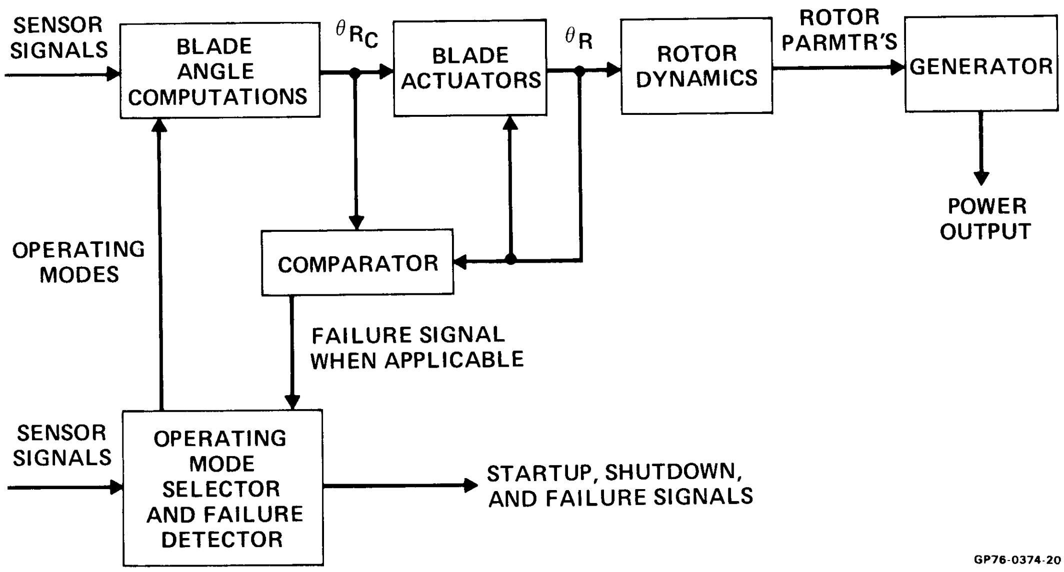

FIGURE 19
GIROMILL CONTROL SYSTEM
FUNCTIONAL DIAGRAM

One of the several Giromill system condition and failure detection control loops is shown. This is a comparison between the commanded rock angle and that actually achieved by the blades. A partial failure or binding of one actuator could occur without effecting any other system parameters since the remaining blades could make up the power difference. By comparing the commanded Θ_{R_C} with the actual achieved Θ_R, and assuring they are within a specified tolerance from each other protects against such a failure. If a failure is detected the mode selector will command a shutdown of the Giromill system. Shutdown is accomplished by declutching the blades from their actuator allowing them to weathervane into the wind. Other system condition and failure detection control loops are: excessive vibration level cut off, high and low wind cut-off, electrical power condition cut off, startup sequencing, normal blade declutching and emergency blade declutching.

The Giromill control system functions are, generally speaking, quite similar to the conventional windmill control system. The main difference lies in the blade rock angle control implementation. The rock angle implementation within the control system was incorporated as shown functionally in Figure 20. The implementation consists of computing the blade rock angle for zero angle of attack and no induced effects (Θ_{R_0}), and successively modifying this rock angle to account for the desired effective angle of attack, (α_e), and the induced angle of attack, (α_i). A generator power condition is fed back to make an incremental blade rock angle correction to keep the power output within specification.

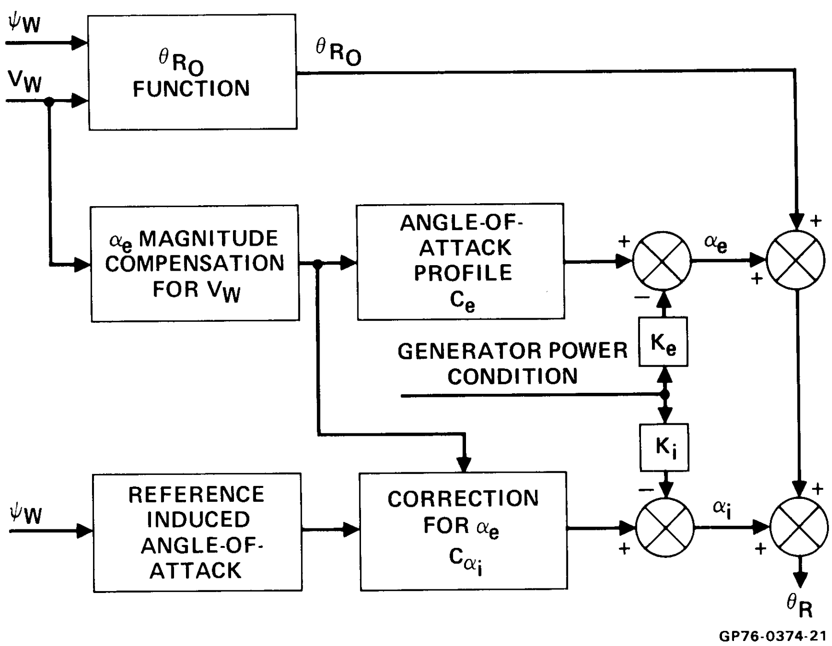

FIGURE 20
BLADE ROCK CONTROL PROCESSOR

The equation that relates the blade rock angle for zero angle of attack assuming no induced effects is:

$$\Theta_{R_0} = \arctan\left[\frac{-\cos\psi}{\frac{\omega R}{V_W} - \sin\psi}\right]$$

where: ψ = Blade phase angle
ωR = Blade rotational speed
V_W = Wind velocity

This computation is denoted by the Θ_{R_0} function block in the diagram of Figure

20. The Θ_{R_O} thus computed is then modified for the desired α_e which is programmed as a function of wind velocity. The angle of attack profile box relates the α_e to a positive or negative value depending on the blade phase angle by multiplying by the coefficient C_e. This then provides a rock angle that would provide the desired blade $\pm\alpha_e$ around the rotor but neglects the induced effects.

The induced effects are determined by using as a reference the induced effects α_i computed by the vortex theory program at the α_e for rated power, and then correcting α_i for the actual α_e being commanded. This correction was determined empirically using the vortex theory program, and takes the form of a multiplying constant, C_{α_i}, determined as a function of the actual $\alpha_e/\alpha_{e_{max}}$ being commanded at that time. This was checked out over the range of wind velocities expected, and predicted quite accurately the expected α_i. Since a smooth reference α_i is used, this also smooths the final Θ_R computed. The results of applying this technique are illustrated in Figures 21, 22, and 23.

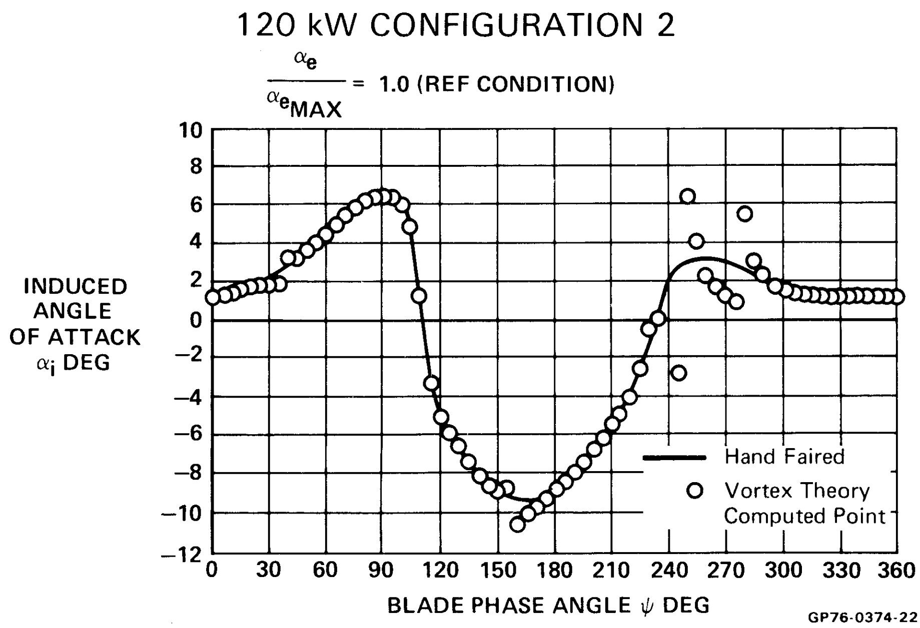

FIGURE 21
INDUCED ANGLE OF ATTACK ALONG THE BLADE ORBIT
120 kW Configuration 2

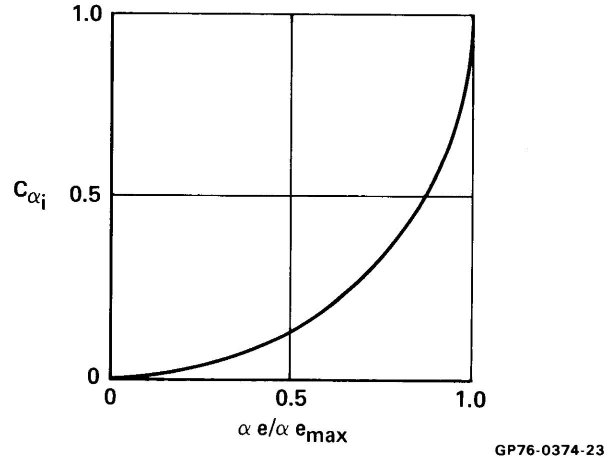

FIGURE 22
INDUCED ANGLE OF ATTACK VARIATION

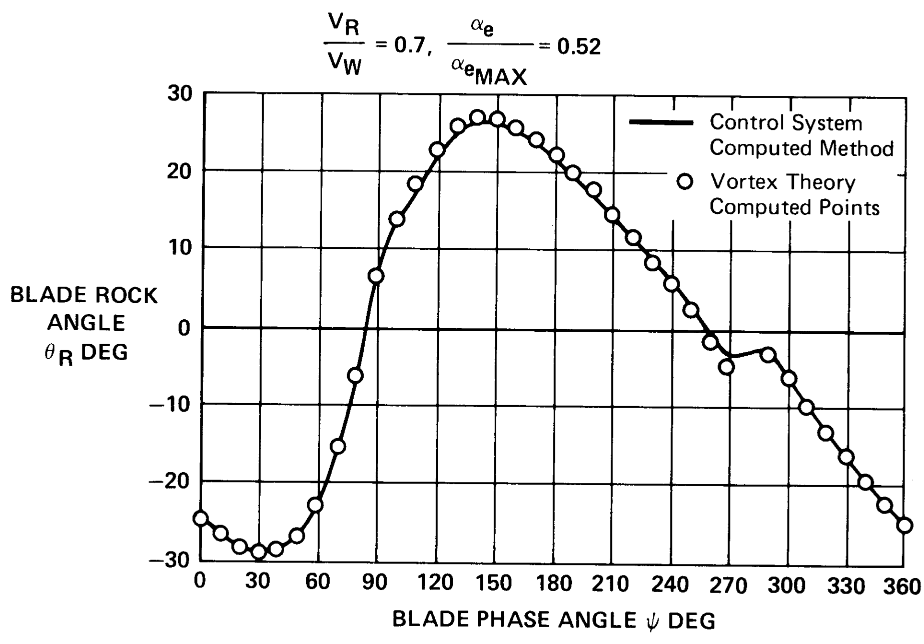

FIGURE 23
ROCK ANGLE COMPUTATION COMPARISON
120 kW Configuration 2

Figure 21 shows the reference induced angle of attack as computed by the vortex theory and smooth hand faired curve. Figure 22 presents how the magnitude of α_i varies in terms of a multiplying coefficient C_{α_i} plotted against the angle of attack ratio $\alpha_e/\alpha_{e_{max}}$. This curve assumes that the nominal α_e to provide for the desired Giromill operation is being commanded. Figure 23 shows a typical example of how well this technique works. This is for a case where $V_R/V_W = 0.7$, and α_e would nominally be 4.7^o to maintain constant power and RPM. $\alpha_{e_{max}}$ for this configuration was 9^o. The power output using this technique was about 9% high, and would be reduced using the generator power condition feedback loop to incrementally correct α_e and α_i to get back to the desired power.

This rock angle control technique has been programmed on the computer and functionally checked out.

8. ENERGY OUTPUT EVALUATION

The Giromill energy output was obtained using the performance characteristics integrated over the wind duration curves. The wind duration curves were for a mean wind of 5.4 mps and 8.1 mps. The 120 and 500 kW systems used the 5.4 mps mean wind curve and the 1500 kW systems the 8.1 mps mean wind curve. These winds are specified at a height of 9 m (30 ft), and have to be uprated to an average height of the Giromill. For simplicity this average height was always taken as 30 m (100 ft). The 1/7 power law for wind velocity with height was used.

9. COST ANALYSIS

The Giromill cost analysis was conducted using ground rules similar to those used for the conventional windmill studies by GE and Kaman. The ground rules used are summarized in Figure 24.

- 1975 DOLLARS
- PRODUCTION COSTS ONLY FOR 100TH UNIT (NO RDT&E)
- ANNUAL RECURRING COSTS
  - COST OF CAPITAL
  - OPERATION AND SUPPORT (O&S)
- OFF-THE-SHELF EQUIPMENT WHEREVER POSSIBLE
- COST ESTIMATING RELATIONSHIPS (CER) DEVELOPED vs PHYSICAL PARAMETERS (SIZE, POWER OUTPUT, RPM, WEIGHT, ETC.)

GP76-0374-28

FIGURE 24
GIROMILL SYSTEM COST ANALYSIS GROUND RULES

One of the major cost components of the Giromill turned out to be the main rotor bearings. The upper main bearing size is dictated by the upper tower diameter because of structural dynamic considerations. The lower main bearing size is dictated by the upper tower end cap design and was assumed to have a diameter of 1.5 meters. The cost estimating relationship used for these bearings is shown in Figure 25.

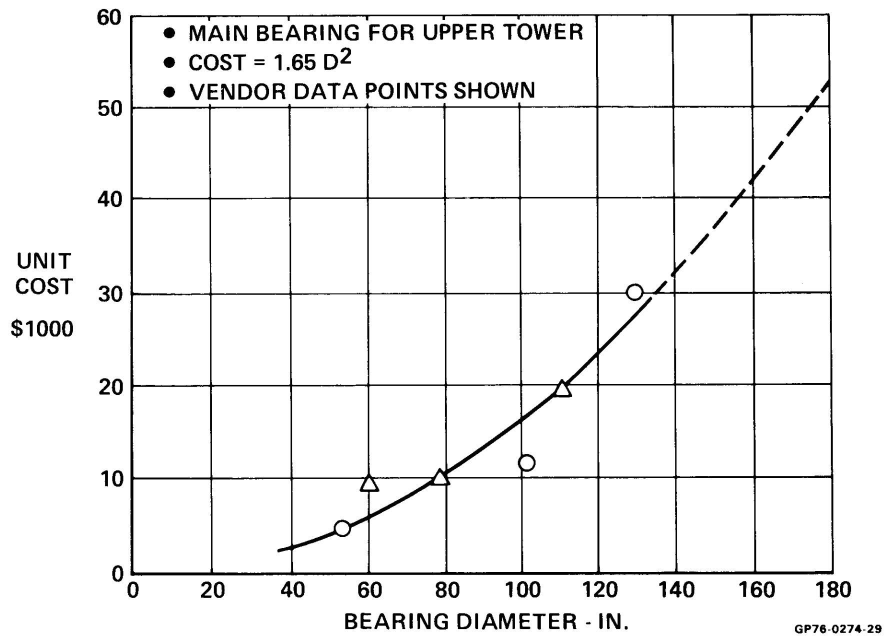

FIGURE 25
COST ESTIMATING RELATIONSHIP (CER) FOR LARGE COMBINATION BEARING

Figure 26 presents a summary of the subsystem and component costs used in the cost analysis. Note that the blade cost factor is \$4.00/lb. This is a consequence of the simple blade design made possible because of the symmetrical untapered and untwisted blade used for the Giromill.

The speed increaser and generator costs were obtained from vendor data, but were increased because of the vertical mounting used with the Giromill. The speed increaser cost was increased 10% and the generator cost 15%.

Other cost elements used are presented in Figure 27. The additional capital costs for final assembly, shipping, land and site development, etc. were based on reference data. The cost of capital was set at 15% of the total installed cost of the Giromill, and covers the following annual charges:

- o Depreciation
- o Cost of indebtedness, interest on bonds and notes
- o Federal income tax
- o State and local taxes
- o Cost of equity, common and preferred stock.

ELEMENT	MATERIAL OR DESCRIPTION	COST FACTORS
TOWER STRUCTURE ROTOR BLADE SUPPORTS FOUNDATION ROTOR BLADES	CARBON STEEL WELDED OR BOLTED TUBULAR CARBON STEEL CONCRETE ALUMINUM	\$0.75/LB \$0.75/LB 25% OF TOWER COST \$4.00/LB
DRIVE SYSTEM COUPLINGS SPEED INCREASER	SPEED INCREASER, GENERATOR DRIVE SHAFT 120 kW 500 kW 1500 kW	\$4 TO \$5/LB \$15,000 TO \$22,000 \$26,500 TO \$33,000 \$48,000
ELECTRICAL SYSTEM GENERATOR	1200 RPM FOR 120 kW RPM VARIES FOR 500 kW SYSTEM 450 RPM FOR 1,500 kW GENERATOR CONTROLS, PANELS, ETC	\$4,025 \$23,000 TO \$27,000 \$58,000 \$4,025
CONTROL SYSTEM ACTUATORS OTHER	THREE REQUIRED 120 kW 500 kW 1500 kW CONTROL SYSTEM SENSORS, ETC	\$2,400 EACH \$3,400 EACH \$4,600 EACH \$10,000

GP76-0374-30

FIGURE 26
SUBSYSTEM AND COMPONENT COSTS

COST ELEMENT	DESCRIPTION	COST FACTORS
ADDITIONAL CAPITAL		
INCIDENTAL COSTS	FINAL ASSEMBLY, SHIPPING, ETC	10% OF TOTAL COST
SITE AND PREPARATION	LAND, SITE DEVELOPMENT, SECURITY - 120 kW	\$15,000
	500 AND 1500 kW	\$30,000
ANNUAL CHARGES		
COST OF CAPITAL	LOAN REPAYMENT, DEPRECIATION, BOND INTEREST, STOCK DIVIDEND, TAXES	15% OF TOTAL CAPITAL
OPERATING AND SUPPORT		4% OF TOTAL CAPITAL
TOTAL		19% OF TOTAL CAPITAL

GP76-0374-31

FIGURE 27
OTHER COST ELEMENTS

This 15% was based on a total financing structure composed of 60% bonds, 10% preferred stock and 30% common stock. The 15% cost of capital agrees well with values used in other current wind power generation programs.

The operations and support costs of 4% considered:

- Salary for maintenance and supervisory personnel
- Insurance
- Maintenance and overhaul costs
- Miscellaneous expendables
- Administrative and general expenses

This value of 4% appeared conservative when compared with the values currently used by the electric utilities, but appears warranted at this time for a new system like the Giromill.

Figure 28 presents some typical results of the production costs for the 500 kW systems. The top 3 values, configurations 13, 9 and 14, show the cost effect of rated wind speed. The last set of values, configuration 11, was the least cost 500 kW Giromill system. These costs are all based on the initial analyses and did not incorporate any cost optimization in the Giromill design. The high cost of the main bearings, especially for the large Giromill system having a low rated wind speed (configuration 13) is evident.

COSTS IN $1000
CONFIG 13, 9, 14
($AR_R = 1.07, \sigma = 0.119$)
CONFIG 11
($AR_R = 0.48, \sigma = 0.079$)

CONFIG NUMBER / $V_R/\overline{V}_W$	TOWER, FOUND. AND BLADE SUPPORT	ROTOR BLADES	ELECTRICAL	DRIVE	MAIN BEARINGS	TOTAL SYSTEM COST*
13/1.33	310	77	31	44	230	723
9/1.50	206	68	29	42	163	538
14/1.67	144	63	27	41	119	424
11/1.50	167	29	31	44	72	373

*Includes $30,400 for Control Systems

GP76-0374-32

FIGURE 28
PRODUCTION COST ELEMENTS 500 kW Giromill

Configuration 11 resulted in the lowest energy cost for a 500 kW system. This system was then subjected to a design optimization effort to bring down the cost of energy. The results of this optimization are shown in Figures 29 and 30. Figure 29 shows the energy cost for the four 500 kW configurations shown in Figure 28, and the optimized configuration 11-1. Note that the energy cost exhibits a trend with rated wind similar to that observed with conventional windmills, i.e., having a minimum energy cost at a rated to mean wind ratio near 1.5. Also note that optimizing the 500 kW system reduced the cost of energy about 28%, from 5.6 to 4.05 ¢/kWH.

Figure 30 shows the least energy cost for the 120, 500, and 1500 kW systems based on the initial design and cost assumptions, and the optimized 500 kW system.

CONFIG NUMBER $\frac{V_R}{\bar{V}_W}$	INSTALLED COST ($1000)	INSTALLED COST ($/kW)	ANNUAL POWER OUTPUT (kWH)	ENERGY COST (CENTS/ kWH)
13/1.33	825	1,651	1,875,000	8.4
9/1.50	622	1,243	1,490,000	7.9
14/1.67	496	993	1,160,000	8.1
11/1.50	441	881	1,490,000	5.6
11-1/1.50 OPTIMIZED	336	671	1,574,000	4.05

GP76-0374-33

FIGURE 29
COST OF ENERGY PRODUCED
500 kW Giromill

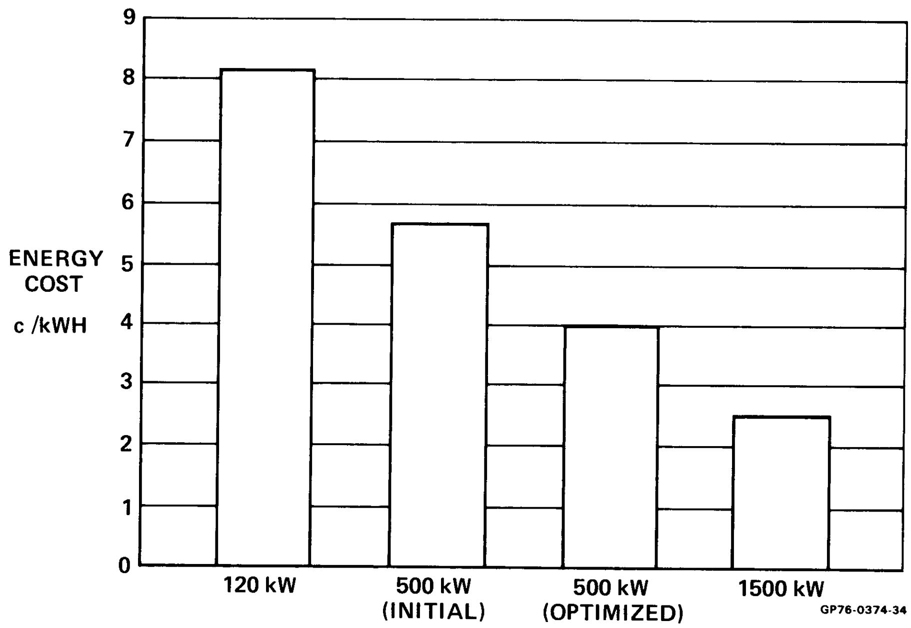

FIGURE 30
GIROMILL ENERGY COST

10. CONCLUSIONS

A parametric design and cost effectiveness analysis of 120, 150, and 1500 kW Giromill systems has been completed. This preliminary analysis shows that the Giromill appears feasible and cost effective. Energy costs of a 500 kW system placed in a 5.4 mps mean wind site are 4.05 c/kWH.